Powder Technology 436 (2024) 119455

Contents lists available at ScienceDirect

Powder Technology

journal homepage: www.journals.elsevier.com/powder-technology

Jet-spouted bed in conical contactor for winery waste drying

María J. San José *, Sonia Alvarez, Raquel López

Departamento de Ingeniería Química, Facultad de Ciencia y Tecnología, Universidad del País Vasco UPV/EHU, Apdo. 644, 48080 Bilbao, Spain

HIGHLIGHTS

- Conical spouted bed dryer is suitable for drying of winery waste.
- The operability of beds of winery waste was determined in the jet-spouted bed.
- Jet-spouted bed regime is highly efficient for drying of winery waste.
- Time evolution of gas humidity was predicted by an artificial neural network.
- Evolution of solid moisture content was obtained from gas humidity by mass balance.

GRAPHICAL ABSTRACT

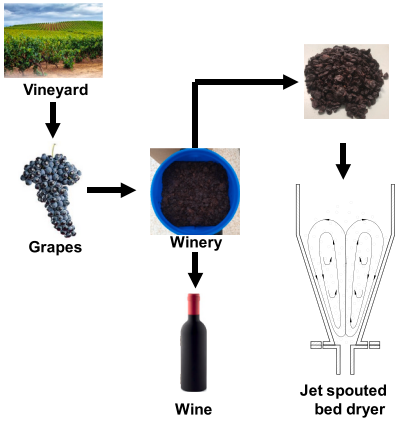

ARTICLE INFO

Keywords:
Conical spouted bed dryer
Drying jet-spouted-bed performance
Drying model
Neural network
Jet-spouted bed (dilute spouted bed)
Winery waste

ABSTRACT

To analyze the performance of a conical spouted bed dryer for the valorization of wine-production waste (grape skins, seeds, and stalks) in a jet-spouted-bed regime (dilute spouted bed), the operating conditions in the jet and spouted-bed regimes were delimited for comparison. Drying was conducted at different air temperatures and velocities in both regimes, and the time evolution of the gas humidity and solid moisture content was monitored to obtain the most appropriate conditions for drying. An artificial neural network was trained to predict the time evolution of gas humidity in both regimes in a conical spouted bed dryer. From these data, the solid moisture content was determined using differential mass and heat balances, considering equal temperatures in the gas and solid phases. Finally, the fitting of the experimental results of the solid moisture content demonstrates the validity of drying tracking from the time evolution of the air humidity.

1. Introduction

The world is facing an unprecedented energy crisis, to which the COVID-19 pandemic and Russia's invasion of Ukraine have contributed [1]. Renewable energies, including biomass, with a share of 15% of the primary energy supply in 2020 [2], play a key role in the transition to clean energy and climate change mitigation [3], contributing to attenuating the effects of the crisis. The use of biomass is recommended to

* Corresponding author.
E-mail address: mariajose.sanjose@ehu.eus (M.J. San José).

https://doi.org/10.1016/j.powtec.2024.119455
Received 1 November 2023; Received in revised form 11 January 2024; Accepted 21 January 2024
Available online 25 January 2024

avoid additional environmental contamination [4]. Biomass has been the primary renewable energy resource worldwide for millennia. In prehistoric times, humankind first started burning wood to cook and stay warm. Currently, 96% of all renewable heat produced worldwide comes from biomass [2]. Woody biomass from forestry is currently the most important biomass resource for energy generation. Other sources include agricultural (energy crops) and waste biomass (agricultural waste, food industry waste such as shells and olive pits, and municipal organic waste) [5].

The common grape vine (*Vitis vinifera*) is a very important fruit crop worldwide, with 7.3 million Ha of cultivated land globally, a global grape production of nearly 7 million tons, and wine production of 258 million hL in 2022 [6]. The wine sector generates a large amount of biomass waste (approximately 20 wt% of the grapes), characterized by high organic content and low concentrations of nitrogen and phosphorus [7]. This waste includes pomace, the main by-product, constituted by skins, seeds, and stalks obtained after the extraction of grape juice [8]; lees precipitates generated in the clarification process of the fermentation and maturation of wine [9]; and vinasse depleted of the wine obtained from the sludge washing water and sewage sludge.

Winemaking waste is usually managed by distilleries or utilized as fertilizer. This renewable energy source could become an important raw material for thermal valorization, as a source of heat for drying waste to a dryness content close to 10–15 wt% and for the heating system of the company. The potential application of winery waste in energy production is affected by its high moisture content. Although winemaking byproducts are a source of natural bioactive compounds with substantial antioxidant potential, they are vulnerable to microbial deterioration because of their high moisture content [10]. Therefore, a pre-drying process provides relevant advantages for combustion by providing higher thermal efficiency (by lowering the concentrations of carbon monoxide) [11], which reduces the flue gas emissions of volatile compounds. Owing to previous drying, transport costs are lower, quality is preserved in storage, stability is improved [12,13], and biological activity is inhibited.

The drying kinetics of grape pomace were studied in an infrared dryer and convective dryer at 90 °C [14]; in an air dryer and accelerated solar dryer at 55 °C [15]; in a tray dryer at 55, 65, and 75 °C [16], and at 60, 65, 70, 75, 80, and 85 °C [17], by non-thermal electrohydrodynamic drying [18]; in a heat pump dryer at 45 °C and different air velocities (1.5, 2.0, and 2.5 m/s) [13], and at 45 and 50 °C with an air velocity of 1.0 m/s [19]; and in an air dryer, vacuum dryer, ultrasound assisted vacuum dryer, and freeze dryer [20]. Although several authors have reported on the drying of winery waste, most studies have focused on the effect of the drying method on the chemical composition, bioactive compounds, and antibacterial activity on a laboratory scale [10,21–27] and on an industrial scale [28].

The combustion performance, the first stage of which is the drying of wine waste, was studied using thermogravimetric analysis [29,30]. Wine pomace has a long combustion time, which is an interesting parameter for fuel, a high heating value, an ash content near 10 wt%, and a CO/CO_2 ratio lower than 10% [29]. Schönnenbeck et al. [31] performed the combustion of pre-dried grape marc and its mixtures with conventional biomass in a domestic boiler, obtaining a $[CO]/([CO] + [CO_2])$ ratio lower than 9%. Benetto et al. [32] assessed the feasibility of producing pellets from grape pomace for heat production owing to its high heating value.

A spouted bed is a technology suitable for the fluid-solid contact of coarse solids, sludge, pastes, sticky or viscous irregular textures with a wide particle size distribution, and mixtures of different particle sizes or densities [33]. The good performance of this technology in operations and processes is based on the vigorous cyclic movement of the solid particles [33]. This provides a high turbulence in the bed, avoiding problems inherent to fluidized beds such as defluidization by agglomeration [34] and segregation [35], and allowing efficient fluid-solid contact, which improves both fluid-solid mass and heat transfer [36–39] relating to fluidized and fixed beds [40]. Moreover, unlike fluidized beds, conical spouted beds do not require the use of inert materials as adjuvants such as sand [41].

In conical spouted beds in the spouted-bed regime, three regions are distinguished: the spout zone, annular zone, and fountain [42]. Beds in spouted-bed contactors with a conical geometry are characterized by two characteristic regimes depending on the fluid flow: the spouted-bed regime and jet-spouted-bed regime [33,43]. The jet-spouted bed regime presents hydrodynamic characteristics that are different from those of the spouted bed [43–46]. This regime provides more vigorous solid movement and better gas-solid contact than the spouted-bed regime. The jet-spouted-bed regime is advisable in operations involving adherent sludge because it promotes higher mass and heat transfer rates, avoids particle segregation, and improves the mixing of particles of different sizes and densities. It also enables uniform operation with wide particle distributions [33,43]. The design factors of the conical contactors and the operating conditions in the jet-spouted-bed regime were delimited in previous studies on glass beads are: $D_o/D_i = 1/2–5/6$ for both spouted bed and jet spouted bed regimes, and $D_o/d_p = 2–60$ in the spouted bed regime, and $D_o/d_p = 1–80$ in the jet spouted bed regime [33,43]. The gas flow pattern was analyzed in the jet-spouted bed regime for materials with different densities and particle diameters in conical spouted beds [46]. The operating conditions for the treatment of sludge waste at high temperatures were delimited in the spouted bed and jet-spouted bed regime in conical spouted beds [47].

Spouted bed technology has been successfully applied to the treatment of biomass waste in the spouted-bed regime by drying [42,48–58], combustion [11,59–63], pyrolysis [64,65], gasification [66–69], and anaerobic digestion [70].

Artificial neural networks (ANNs) have been effectively used to predict the behavior of certain materials in spouted beds. Freire et al. [71] used a hybrid lumped parameter/neural network model to estimate the outlet air temperature, relative humidity, air temperature, and material moisture content as functions of time during the drying of pastes with inert particles. A hybrid neural network was also used to estimate changes in moisture content during milk drying [72]. The pressure drop and minimum spouting velocity evolution during the drying of skim milk were predicted using an ANN [73]. A hybrid model consisting of an ANN coupled with a phenomenological model was used to simulate the time evolution of the particle diameter and density, solid moisture content, and gas humidity during the drying of guava [74].

There is a lack of literature regarding the application of the jet-spouted-bed regime for drying; therefore, in this study, a conical spouted-bed contactor was designed for the drying of beds consisting of mixtures of winery waste (grape skins, seeds, and stalks) in the jet-spouted-bed regime. The operability of the winery waste mixture beds in the jet-spouted-bed regime was determined by the evolution of the bed pressure drop with air velocity [75], whose maximum pressure drop determines the impulsion equipment. Similarly, the drying performance of winery waste was studied in the jet-spouted-bed regime under different operating conditions of air velocity and temperature. Furthermore, an ANN model was developed and trained to predict the drying kinetics of winery waste and the evolution of gas humidity and solid moisture content over time in the jet-spouted-bed regime in a conical spouted-bed dryer.

2. Materials and methods

2.1. Equipment

The experimental equipment, previously designed at the pilot plant scale and shown in Fig. 1, has been described in detail in the literature [11,52]. It consisted of a conical reactor, an impulse blower, a high-efficiency cyclone to retain fine particles, and a mass flow meter (accuracy ±0.5%) controlled by a computer that measured the air flow rate inside an extractor hood.

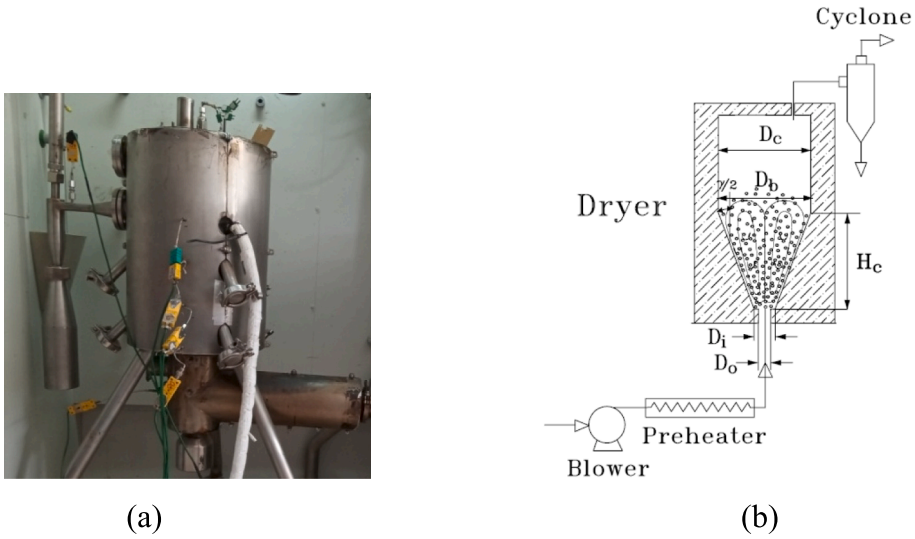

Fig. 1. (a) Experimental equipment and (b) scheme, along with the geometry of the conical spouted bed rector and the particles of winery waste in the jet-spouted bed regime.

The conical spouted bed dryer (Fig. 1) was made of 316 stainless steel. It had an angle of 36°, base diameter of 0.03 m, and inlet fluid diameter to inlet dryer diameter ratios D_o/D_i of 1/2, 2/3, and 5/6. The geometric factors of the conical dryer are depicted in Fig. 1, along with an overview of the solid particles in the jet-spouted bed regime. The upper part of the conical dryer was a 10× methacrylate magnifying glass that allowed visualization of the bed from the outside.

The air flow provided by the blower was heated by an electrical heater specifically made for the purpose (Reyter, Spain), located horizontally before the dryer, controlled by Selecta Electemp-TFT (J.P. Selecta, Spain, accuracy ±0.1 °C), based on a set temperature measured by a K-type thermocouple (relative error of ±0.75% or ± 2.2 °C) placed at the dryer inlet. Electrical heaters were installed around the external wall surface of the dryer to reduce heat loss. These heaters were controlled by a Schneider Electric controller (France, accuracy ±0.5%) using the temperature determined by a thermocouple, which could be adjusted to various positions inside the dryer. Quartz fiber was used to insulate the heaters, and the reactor was encased in a cylindrical jacket made of AISI-310S stainless steel. K-type thermocouples were used to measure the air temperatures at various longitudinal and radial angles within the dryer throughout the drying process. The air temperature and humidity content at both the inlet and outlet of the dryer were monitored by Alhborn MT8636-HR6 thermal conductivity detectors (Ahlborn, Germany, accuracy ±2% relative humidity). The data stored in the Alhborn Almemo 2290–8 data logger are important control parameters for the drying performance. The temperature of the solid was measured using an infrared laser thermometer (Fluke 572–2, USA).

2.2. Materials

The biomass used was winery waste consisting of grape skins, seeds, and stalks obtained during the pressing of grapes to obtain grape juice (Fig. 2), with a density of 1050 kg/m^3, a particle size ranging from 13 to 7 mm, belonging to the D Geldart group, and a moisture content of 150 wt% (dry basis) measured by the Mettler Toledo HB43-S Halogen hygrometer (Mettler Toledo, Switzerland, accuracy ±0.01%). This method of moisture measurement was previously checked by drying samples in an oven at 105 °C for 24 h (ISO 18134-1:2015 standard). "In order to uniformize the size and the shape the winery wastes were ground to smaller particle sizes by the Fritsch Pulverisette 15 mill (Fritsch, Germany) and sieved by meshes in a sieving machine (Filtra FTI-0300, Filtra Vibracion, S.L., Spain), obtaining 5–6 mm particles with a Sauter mean diameter of 5.6 mm, equivalent sphericity of 0.9, and stagnant bed

Fig. 2. Particles of winery waste (grape skins, seeds, and stalks). Wet particles are left of the diagonal, dry particles right of the diagonal.

porosity of 0.64. Gas inlet diameter to Sauter mean diameter ratio, D_o/d_p, is 5.36, which is comprised within the ranges of the geometric factors corresponding to the spouted bed and jet-spouted bed regimes of the design factors of conical spouted beds reactors [43]."

Particles from the winery waste bed were sieved before and after each drying experiment to determine whether there was a size variation due to attrition.

2.3. Drying

The moist winery waste was dried in a conical spouted bed dryer under two operating regimes:

- in the jet-spouted bed regime from the minimum jet-spouting velocity to 1.5 times greater than the minimum
- in the spouted-bed regime from 2% above the minimum spouting velocity (to ensure that it is in the spouted-bed regime and prevent the fountain from collapsing owing to a small change in the air flow provided by the blower) to 1.5 times greater than the minimum

with inlet air temperatures ranging from 40 to 105 °C, and a bed mass of 50 g. Temperatures below 40 °C were not used because drying times are long and generate a certain attrition which separates the seeds from the skin without segregation and with insignificant elutriation (<1 wt%).

Drying air, consisting of hot flue gas from a blower heated after passing through an electrical heater, was used to preheat the conical dryer to the desired temperature before feeding the biomass. All experiments started with identical gas absolute humidity (0.007 ± 2% kg water/kg dry air) and solid moisture content (150 ± 0.01% dry basis) to ensure that the drying results were comparable.

In the drying experiments of beds consisting of winery waste in a conical spouted-bed dryer, the air relative humidity and temperature at the exit were monitored with time until the air humidity remained almost constant and equal to that of the inlet. The absolute humidity (Y) of the air was obtained from the relative humidity and temperature. Simultaneously, small solid samples (approximately 0.5 g) were collected from the fountain at regular time intervals using a pump to determine the moisture content evolution of the solids. When the air humidity and solids moisture content difference between two consecutive measurements were lower than 0.05 wt%, the drying process was concluded. Each drying experiment was repeated three times under the same conditions, and the average values were calculated.

3. Results and discussions

3.1. Performance in conical jet-spouted-bed regime

The operating conditions of the beds were determined to dry winery waste (grape skins and stalks) in conical spouted beds in the jet-spouted bed regime.

The delimitation of the operating regimes of beds consisting of winery waste from the fixed bed to the spouted-bed and jet-spouted bed regimes was determined by the evolution of the bed pressure drop with air velocity, u, referred to as the diameter of the dryer bottom, D_i. The bed pressure drop increased as fluid velocity increased from zero to the maximum pressure drop value, then sharply dropped until a stable pressure drop was reached. The fluid velocity continued increasing until the spouted bed regime was reached (Fig. 3a) characterized by pressure drop fluctuations with a standard deviation <10 Pa [75], which remained constant over a range of air flows. A velocity increase of 50% allowed operation in the spouted bed regime, while maintaining a constant pressure drop. Subsequently, the bed pressure drop decreased gradually until it reached the jet-spouted bed regime (Fig. 3b) at the minimum jet-spouted bed velocity, after which it did not remain constant. The minimum spouting velocity, u_{ms}, was obtained by decreasing the air flow rate until the fountain disappeared. By decreasing the fluid velocity, the pressure drop was lower than that measured by increasing the fluid velocity owing to hysteresis.

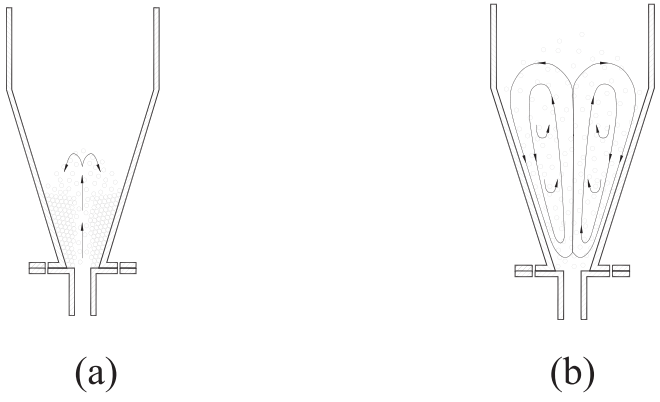

Fig. 3. Outline of particle movement in the (a) spouted-bed regime and (b) jet-spouted-bed regime.

For various masses corresponding to the stagnant bed height to height of the cone section ratio, H_o/H_c, as air velocity increased, the experimental values of the gas velocity ranges corresponding to the spouted-bed and jet-spouted-bed regimes were determined for air temperatures ranging from 40 to 105 °C. Table 1 lists the air velocity ranges corresponding to the spouted-bed and jet-spouted bed regimes for a bed consisting of winery waste at 105 °C as an example. The operating zone in the jet-spouted bed regime was larger than that in the spouted bed regime at every stagnant bed height. An increase in the ratio of the stagnant bed height to the height of the cone section led to an increase in the minimum spouting velocity.

The bed voidage, ε, of the beds of winery waste was high; in the spouted bed regime, the voidage increased with increasing gas velocity, from that corresponding to the minimum spouting velocity of approximately 0.70 to the beginning of the jet-spouted-bed regime of approximately 0.97. As the air velocity increased in the jet-spouted bed regime, the bed voidage of winery waste increased sharply from the minimum jet-spouting velocity higher than 0.97 to almost 1, which provided a very vigorous movement of the particles, resulting in a homogeneous gas-solid contact and high mass transfer in the drying process [46].

3.2. Drying of beds consisting of winery waste

Figs. 4–8 demonstrate the experimental results of the time evolution of the air absolute humidity, Y, and the solid moisture content, X, during the drying process of beds consisting of winery waste (grape skins, seeds, and stalks) with a Sauter mean particle diameter of 5.6 mm from the initial solid moisture content of 150 wt% (db) to the equilibrium moisture content with a constant outlet and inlet air humidity.

3.2.1. Effect of air flow rate in the jet-spouted bed regime

Fig. 4a presents the time evolution of the absolute humidity in the drying of winery waste in the jet-spouted bed regime at the minimum jet-spouting velocity (corresponding to 4.2 u_{ms}) and at 1.5 times greater than the minimum jet-spouting velocity (1.5 u_{mj} corresponding to 6.3 u_{ms}) at 105 °C. The dotted lines in Fig. 4a show the experimental values of the absolute humidity of the air for better visualization. The absolute air humidity increased from the inlet air humidity to a maximum value, followed by a decline which asymptotically approached the inlet air humidity. It is worth highlighting that the air flow rate was sufficiently high to avoid saturation of the outlet air humidity and to provide a driving humidity gradient. This behavior occurred in the jet-spouted-bed regime as well as in the spouted-bed regime in conical spouted bed contactors. An increase in the air flow rate from the minimum jet-spouting velocity to 1.5 times the minimum jet-spouting velocity resulted in narrower peaks with higher maximum air humidity values obtained at shorter times. Furthermore, the drying time was considerably reduced.

The time evolution of the solid moisture content of the winery waste in the jet-spouted bed regime at 105 °C is plotted in Fig. 4b. The drying of winery waste occurred during the falling rate drying period, and the constant drying rate period was negligible at the air temperatures studied, as previously reported for the drying of grape pomace in a tray dryer [17] and food products and agricultural grains in spouted beds [48,52,76,77]. The initial induction stage contributed very little to the

Table 1
Experimental values of the gas velocity ranges corresponding to each operating regime at 105 °C.

H_o/H_c	u_s (m/s) range	u_j (m/s) range
0	0	0
0.07	3.25–14.41	14.84–60
0.13	4.91–21.19	22.04–60
0.20	6.98–28.74	29.89–60
0.27	9.29–36.20	37.65–60
0.33	11.35–44.38	45.14–60

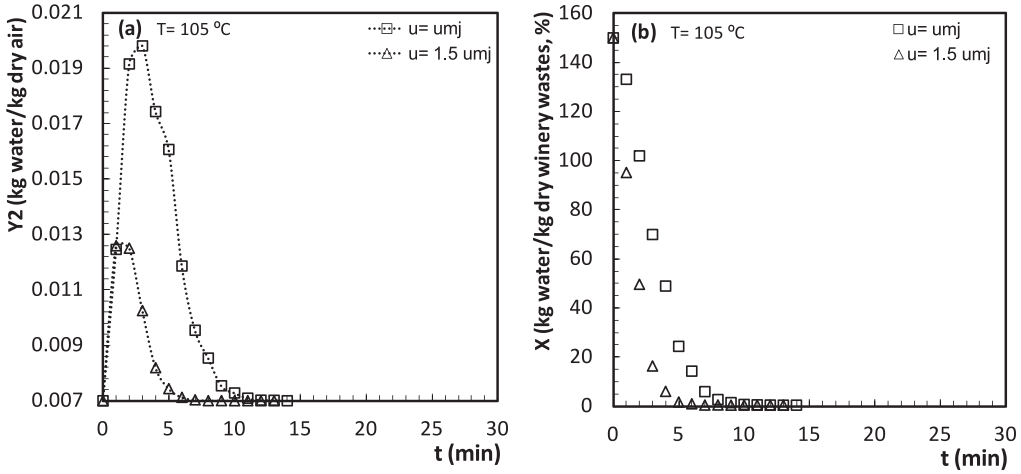

Fig. 4. (a) Time evolution of the outlet air humidity. (b) Time evolution of the solid moisture content. Experimental system: $\gamma = 36°$, $D_o = 0.03$ m, beds of winery waste of M = 50 g, $T = 105$ °C, in the jet-spouted-bed regime u = 1.0, 1.5 u_{mj}.

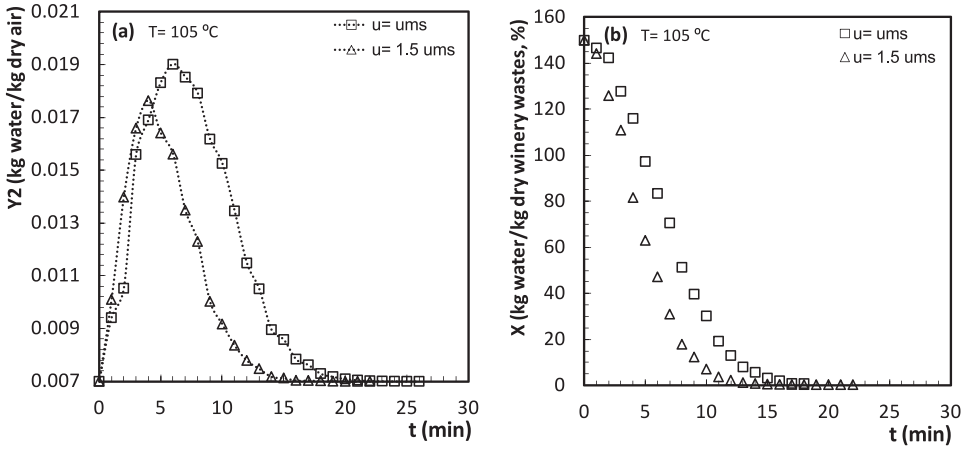

Fig. 5. (a) Time evolution of the outlet air humidity. (b) Time evolution of the solid moisture content. Experimental system: $\gamma = 36°$, $D_o = 0.03$ m, beds of winery waste of M = 50 g, $T = 105$ °C, in the spouted-bed regime u = 1.02 and 1.5 u_{ms}.

drying kinetics, as it lasted only a few seconds owing to the quick heating of the solid by convection. First, the solid moisture content declined proportionately, but later, the decline in moisture content was less than proportional, depicting an asymptotic tendency near the equilibrium moisture content. Increasing the airflow rate in the jet-spouted bed regime led to a higher mass transfer rate, which resulted in a shorter drying time.

The time required to accomplish drying in the jet-spouted bed regime was reduced by around 50% at 105 °C (from 10 to 5 min) from the minimum jet-spouting velocity to 50% greater than this velocity. It is worth mentioning that the minimum jet-spouting velocity, u_{mj}, was achieved at a velocity that was approximately 4.2 times the minimum spouting velocity.

3.2.2. *Effect of air flow rate in the spouted-bed regime*

The results of drying beds of winery waste in the spouted-bed regime are shown in Fig. 5 at 105 °C as an example. In the spouted-bed regime at 105 °C at the minimum spouting velocity and 1.5 × above this velocity, the shape of the curves of the evolution of the air absolute humidity (Fig. 5a) and of the solid moisture content (Fig. 5b) with drying time were similar to those observed in the jet-spouted-bed regime. Nevertheless, the drying times were shorter in the jet-spouted-bed regime, as can be observed from a comparison of Figs. 4 and 5. The drying time decreased by approximately 27% (from 15 to 11 min) as the airflow rate increased from the minimum spouting velocity (1.02 u_{ms}) to 50% greater than the minimum velocity (1.5 u_{ms}).

The effect of the airflow rate on the drying time was similar to that previously observed in drying in conical spouted beds in the spouted bed regime of beds consisting of sludge waste [51] and sawdust [52], grains and vegetables in conventional spouted beds [49,50,77], sawdust in fluidized beds [78], and in a tray dryer [79]. The influence of air velocity on drying time was also in agreement with the results found by Taseri et al. [13] for grape pomace, with a drying time decrease of 69% when the velocity increased from 1.5 m/s to 2.5 m/s.

The drying times were shorter in the jet-spouted bed regime, indicating that they might play an interesting role in the drying of winery waste. A short drying time is of particular interest because it increases the production rate and saves energy, as drying consumes between 15 and 20% of industrial energy [52,80]. Similarly, avoiding over drying is recommended because it reduces productivity and increases energy consumption.

3.2.3. *Effect of air temperature*

The influence of air temperature on the drying behavior of winery waste beds (grape skins, seeds, and stalks) is illustrated in the jet-spouted bed (Fig. 6) and spouted bed regimes (Fig. 7). An increase in drying temperature from 40 to 105 °C reduced the drying time in the jet-spouted-bed regime (Fig. 6) by around 84% (from 62 min at 40 °C to 10

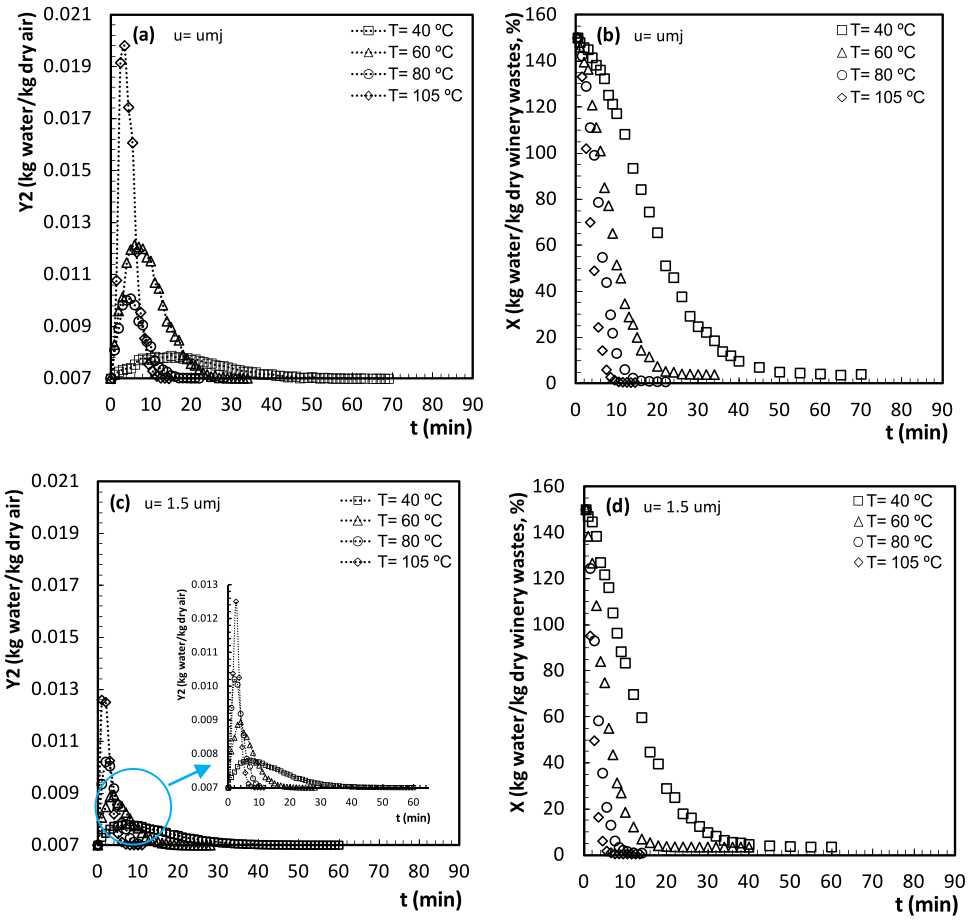

Fig. 6. Time evolution of the outlet air humidity: (a) u = 1.02 u_{mj}, (c) u = 1.5 u_{mj}. Time evolution of the solid moisture content: (b) u = 1.02 u_{mj}, (d) u = 1.5 u_{mj}. Experimental system: γ = 36°, D_o = 0.03 m, beds of winery waste (grape skins, seeds, and stalks) of M = 50 g, *T* = 40, 60, 80, and 105 °C in the jet-spouted bed regime.

min at 105 °C) at the minimum jet-spouting velocity and by about 76% (from 42 min at 40 °C to 5 min at 105 °C) at 1.5 times the minimum jet-spouting. In the spouted-bed regime (Fig. 7) the drying time decreased by around 82% (from 82 min at 40 °C to 15 min at 105 °C) at the minimum spouting velocity and by around 85% (from 72 min at 40 °C to 11 min at 105 °C) at 1.5 times the minimum spouting velocity. The drying time decreased in approximately the same proportion in the jet-spouted-bed regime as in the spouted-bed regime, even though the drying times in the jet-spouted-bed regime were shorter.

The influence of temperature on the drying time was the same as that in the literature, and the drying times were of the same order as those in drying in conical spouted beds in the spouted bed regime of bed sludge waste [51] and sawdust [52] and in conventional spouted beds in the spouted bed regime of agricultural and vegetable materials [49,50,53,76,77,81,82]. In addition, the drying time decreased with temperature during the drying of grape pomace in a heat pump dryer [19].

To find the best option for drying winery wastes, a comparison of the time evolution of gas humidity and solid moisture content was conducted under the highest and lowest air temperatures, 40 and 105 °C, and air velocity u = 1.02 u_{ms} and 1.5 u_{mj} (Fig. 8). Although the shortest drying time of beds consisting of winery waste was obtained at 105 °C in the jet-spouted-bed regime at 1.5 times the minimum jet-spouting velocity, that obtained at 60 °C (Fig. 8b, d) was quite low and similar to that obtained in the spouted-bed regime at the minimum spouting velocity at 105 °C. In addition, the drying time in the jet-spouted-bed regime at 1.5 times the minimum jet-spouting velocity at 40 °C was approximately equal to that obtained in the spouted-bed regime at the minimum spouting velocity at 60 °C (Fig. 8b, d).

The drying times obtained in both the spouted-bed and jet-spouted-bed regimes were shorter than those obtained in other dryers at temperatures below the water evaporation point. The drying time of grape pomace was over six times longer (180–240 min) in an air dryer (at 55 °C) [15], between 8 and 40 times longer (300–1560 min) in an air dryer at 60–85 °C [17], between 15 and 25 times longer (720–1040 min) in an open loop laboratory pilot heat pump dryer [13] at air velocities of 1.5, 2.0, and 2.5 m/s, and the drying time ranged from 17.5 to 72 h for air drying, vacuum drying, ultrasound assisted vacuum drying, and freeze drying [20].

Actually, in the conical spouted bed dryer, the drying times in the jet-spouted bed regime were shorter than in the spouted bed regime because of the vigorous movement of the particles and high bed voidage. The drying time decreased by 1/8th as the temperature increased from 40 to 105 °C and by 1/2 as the air velocity increased from the minimum jet-spouting velocity to 1.5 times that at 105 °C.

The drying time in the spouted-bed regime was reduced by a fifth as the air temperature increased from 40 to 105 °C and by about a quarter as the air velocity increased from the minimum spouting velocity to 1.5 times the minimum spouting velocity at 105 °C.

3.2.4. *Modeling the drying behavior of winery waste*

The drying behavior of winery waste beds (grape skins, seeds, and stalks) in the jet-spouted-bed regime in conical spouted beds at temperatures ranging from 40 to 105 °C was modeled from experimental data using an ANN. This ANN consisted of a three-layer neural network of interconnected neurons, with an input layer with three neurons

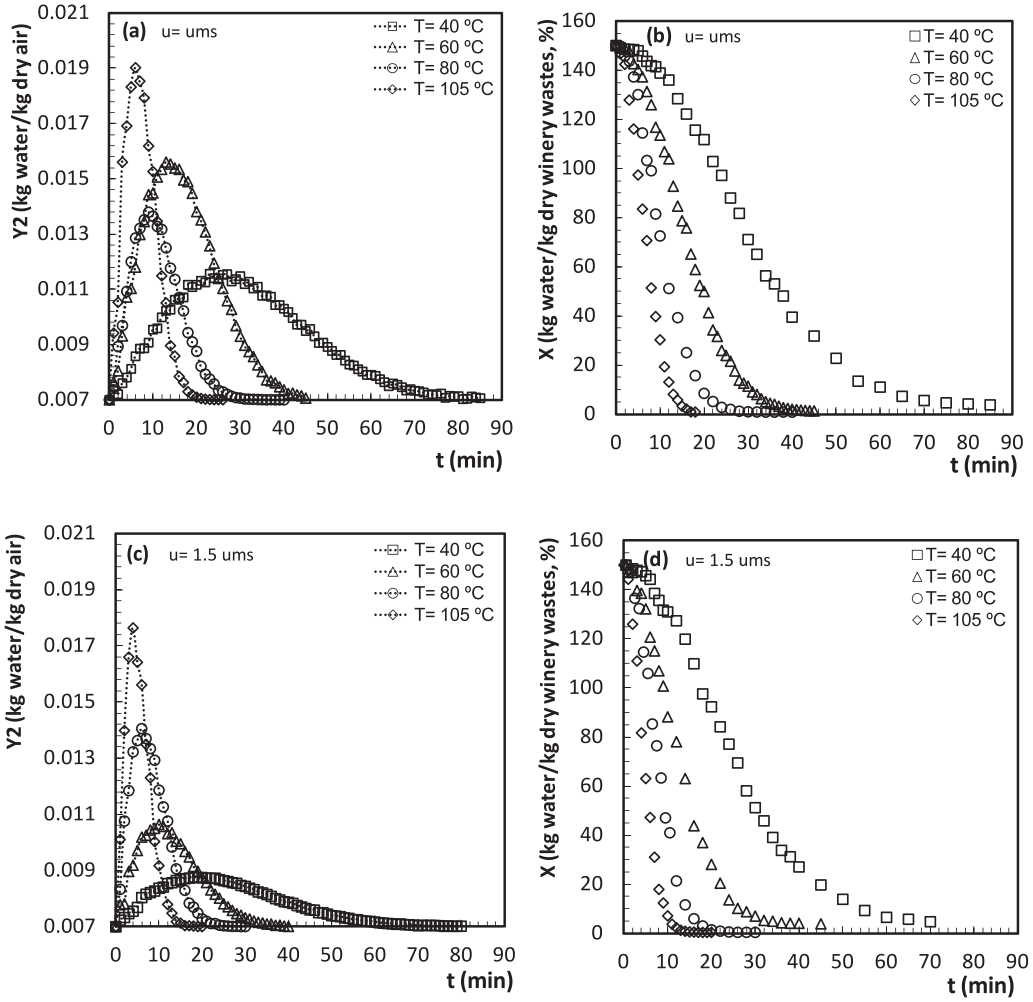

Fig. 7. Time evolution of the outlet air humidity: (a) u = 1.02 u_{ms}, (c) u = 1.5 u_{ms}. Time evolution of the solid moisture content: (b) u = 1.02 u_{ms}, (d) u = 1.5 u_{ms}. Experimental system: γ = 36°, D_o = 0.03 m, beds of winery waste (grape skins, seeds, and stalks) of M = 50 g, *T* = 40, 60, 80, and 105 °C in the spouted-bed regime.

(operating conditions: air temperature, gas velocity ratio to minimum spouting velocity, and time), one hidden layer with 10 neurons, and an output layer with one neuron, gas humidity (Fig. 9), to predict the time evolution of gas humidity. The ANN was developed and trained using the Neural Net Fitting software MATLAB 2022a with the Levenberg-Marquardt and Bayesian Regularization training algorithms. The optimal number of neurons in the hidden layer was determined by trial and error, as suggested by Himmelblau [83], starting with 10 neurons and analyzing the network performance until the number of hidden layers that minimized the root mean square error (RMSE) value was obtained. Fig. 10 shows a schematic diagram of the neural network used in this study. In the development and training of the neural network, a total of 726 data were managed: 395 in the spouted bed regime and 331 in the jet-spouted bed regime. The train ratio for the Levenberg-Marquardt algorithm was 70%, the validation ratio was 15%, and the test ratio was 15%. For the Bayesian Regularization algorithm, the train ratio was 85% and the test ratio was 15%.

The experimental values of the time evolution of the outlet air humidity and the values estimated by the ANN in the drying of winery waste beds are compared in Fig. 11a by the Bayesian Regularization training algorithm and in Fig. 11b by the Levenberg-Marquardt algorithm. The prediction of the gas humidity values provided by the neural network was in good agreement with the experimental results, with values of the correlation coefficient, R, for training, validation, and testing higher than 0.92, and low RMSE (Table 2), with better agreement for the Bayesian Regularization training algorithm than for the Levenberg-Marquardt algorithm.

The evolution of the outlet air humidity over time was a good indication of the drying performance and of how close the solid moisture content was to equilibrium, which was easily monitored by sensors located both at the inlet and exit of the dryer. This avoided bed disruption during the drying process when taking solid samples to measure the evolution of the solid moisture content over time.

Once the time evolution of the outlet air humidity was determined, the time evolution of the solid moisture content could be calculated using a model based on the differential mass balance of the moisture for the solid (Eq. (1)), and the gas (Eq. (2)); Mujumdar [84] considered the equation for the temperature in the gas and solid phases:

$$M_s\, dX/dt = -w_D\, A \tag{1}$$

$$G_s\, dY/dt = G^{\bullet}_s\,(Y_{in} - Y) + w_D\, A, \tag{2}$$

$$\text{where } w_D \text{ is the drying rate} = K\,(Y^* - Y) \tag{3}$$

The global mass transfer coefficient was calculated from the water mass flow and the logarithmic mean concentration difference of the experimental values of air humidity based on the total surface area of the particles [85].

$$K = m^{\bullet}{}_v/(a_o\, V_o\, \Delta Y_m) \tag{4}$$

where $m^{\bullet}_v$ was calculated from the water balance

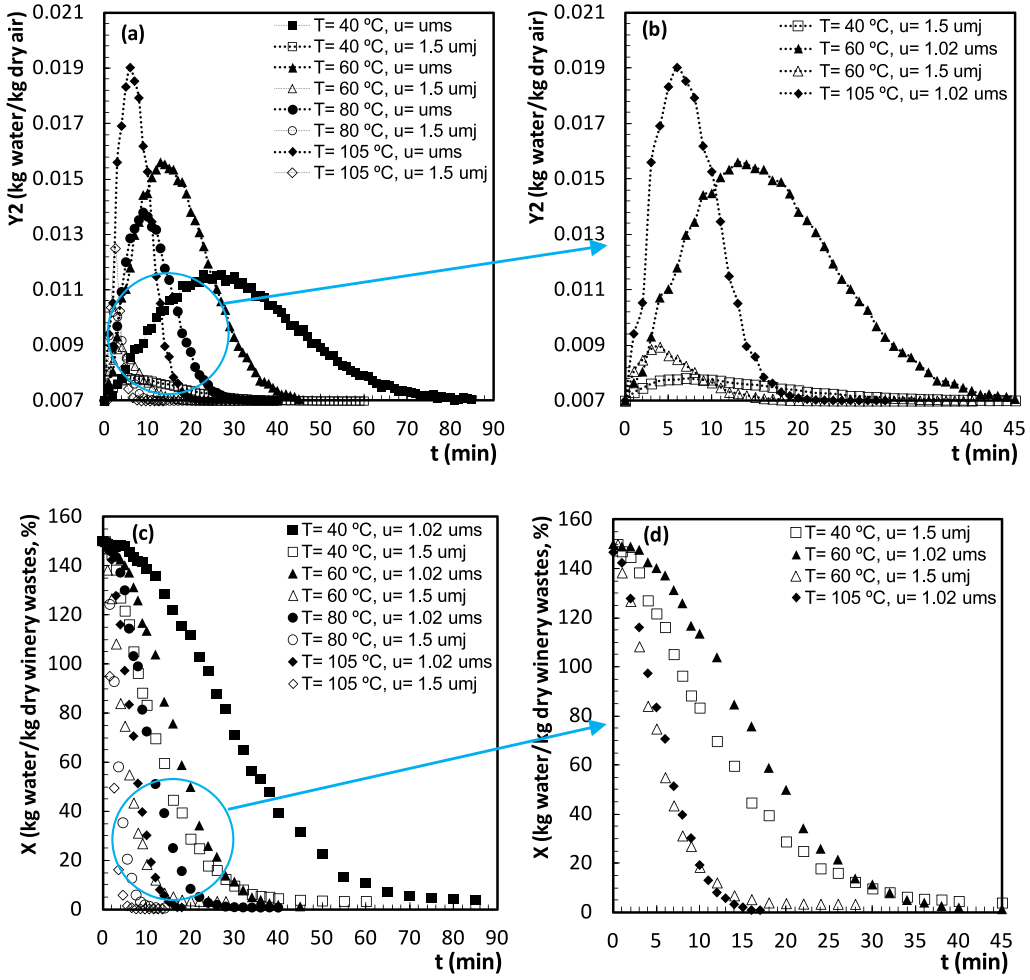

Fig. 8. Time evolution of the outlet air humidity: (a) $T = 40$, 60, 80, and 105 °C, (b) T = 40, 60, and 105 °C. Time evolution of the solid moisture content: (c) T = 40, 60, 80, and 105 °C, (d) T = 40, 60, and 105 °C. Experimental system: $\gamma = 36°$, $D_o = 0.03$ m, beds of winery wastes (grape skins, seeds, and stalks) of M = 50 g, in the spouted-bed regime u = 1.02 u_{ms}, and in the jet-spouted-bed regime u = 1.5 u_{mj}.

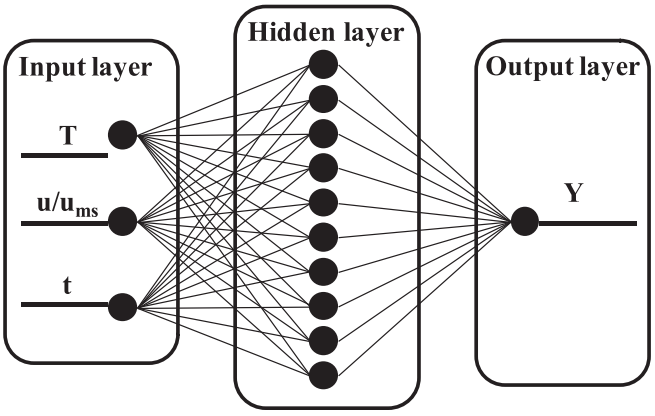

Fig. 9. Schematic diagram of the neural network used to estimate drying behavior of beds of winery waste.

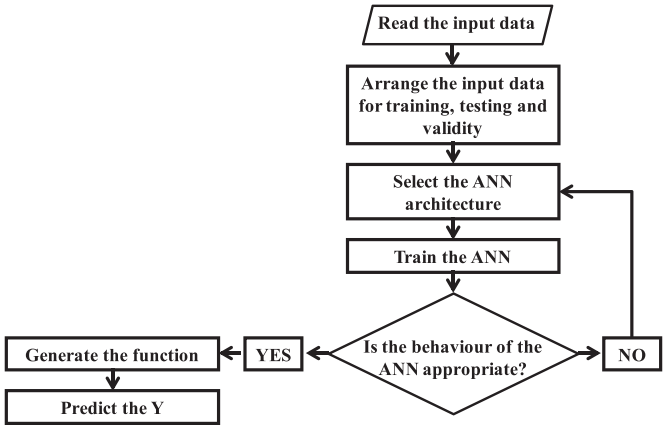

Fig. 10. Flowchart of the algorithm used to develop a neural network to estimate the time evolution of the outlet air humidity in drying beds of winery waste.

$$m^{\bullet}_{v} = G^{\bullet}_{s}\,(Y_2 - Y_1) \tag{5}$$

and ΔY_m is the logarithmic mean concentration difference of gas humidity:

$$\Delta Y_m = Y_2\,\rho_2 - Y_1\,\rho_1 / ln((Y^{*}\rho^{*} - Y_1\,\rho_1)/(Y^{*}\rho^{*} - Y_2\rho_2)) \tag{6}$$

Fig. 12 shows the goodness of the fit of the experimental time evolution values of the solid moisture content (points) to the data determined by the mass balance (lines) for a system taken as an example for the drying of winery waste at 80 °C in the spouted-bed and jet-spouted bed regimes with a high correlation coefficient, ($R > 0.99$), and a maximum relative error lower than 7%.

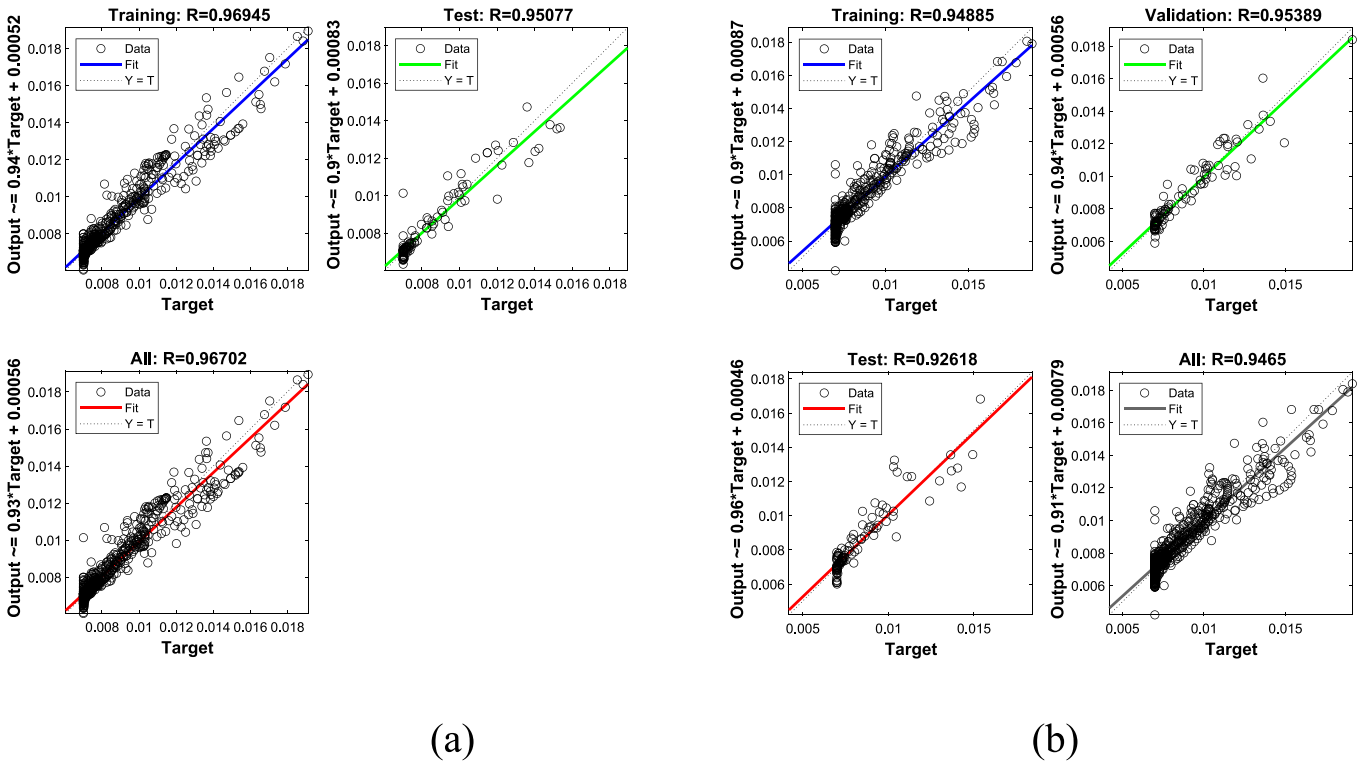

Fig. 11. Model training and testing results of the time evolution of the outlet air humidity by (a) the Bayesian Regularization training algorithm and (b) the Levenberg-Marquardt training algorithm in the drying of winery waste beds.

Table 2
Performance indices obtained by the ANN model for the training, testing, and validation data.

Database	*Bayesian Regularization*		*Levenberg-Marquardt*	
	R	RMSE	R	RMSE
Training	0.96945	$2.407\ 10^{-7}$	0.94885	$1.799\ 10^{-6}$
Validation			0.95389	$2.98\ 10^{-5}$
Testing	0.95077	$2.206\ 10^{-5}$	0.92618	$1.18\ 10^{-4}$
All	0.96702		0.94650	

4. Conclusions

The regimes of the jet-spouted bed and spouted bed consisting of waste from the winemaking process (grape skins, seeds, and stalks) were delimited, and the operating conditions were determined at air inlet temperatures ranging from 40 to 105 °C from the experimental measurements of gas velocity, bed voidage, and the regime characteristics.

The good performance of the conical spouted bed dryer was demonstrated for the drying of winery waste beds in the jet-spouted bed regime, and it was compared with that of the spouted-bed regime. The conical spouted-bed dryer performed well during drying.

The drying of winery waste in the jet-spouted-bed regime led to a reduction in drying time compared to the spouted bed regime in the same temperature range. The jet-spouted bed regime promotes a reduction of 33% in the drying time, at the minimum jet-spouted bed velocity. The highest drying time reduction in the jet-spouted bed regime was 55% at 1.5 times over the minimum velocity necessary to achieve the corresponding regime.

Combinations of temperature and velocity variables were compared in the spouted-bed and jet-spouted bed regimes, and it was determined that the influence of the regime increased as the air temperature increased. The pairs of combinations of temperature and velocity in which the drying efficiency was better were at 1.5 times the minimum jet-spouting velocity at 60 °C and 1.5 times the minimum jet-spouting velocity at 40 °C. Therefore, the jet-spouted-bed regime is the most important regime to use in conical spouted beds for drying winery waste.

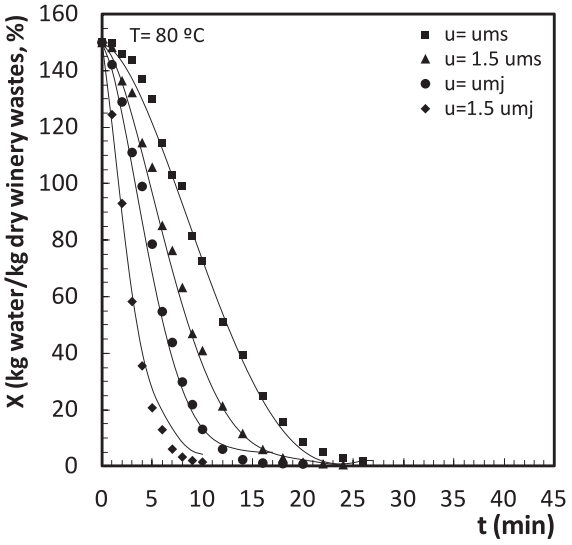

Fig. 12. Time evolution of the solid moisture content. Experimental system: $\gamma = 36°$, $D_o = 0.03$ m, beds of winery waste of M = 50 g, in the spouted bed regime u = 1.0, 1.5 u_{ms}, and in the jet-spouted-bed regime u = 1.02, 1.5 u_{mj}. Experimental values are points, calculated values are lines.

A predictive ANN model was used to predict the time evolution of gas humidity in the jet-spouted and spouted-bed regimes in a conical spouted-bed dryer, which, after training, had good agreement with a correlation coefficient, R, above 0.92.

Tracking the drying performance is suitable for monitoring the evolution of air humidity over time. A model based on the differential

balances of mass based on the literature [84] was proposed, from which the results of the time evolution of the solid moisture content were obtained. These results are in good agreement with the experimental values of solid moisture content. The global mass transfer coefficient obtained from the water mass flow and experimental values of air humidity was of a greater order in the jet-spouted-bed regime than in the spouted bed regime.

Nomenclature

A	bed interfacial area of phase contact (m^2)
Ar	Archimedes number, $Ar = g\ dp^3\ \rho\ (\rho_s\text{-}\rho)/\mu^2$
a_o	particle surface area-to-volume ratio (m^2/m^3)
D_b, D_c, D_i, D_o	diameters of the top of the stagnant bed and the upper diameter of the cone, dryer bottom, and gas inlet, respectively (m)
d_p	particle diameter (mm)
$\overline{d_S}$	Sauter mean diameter (m)
G_s	mass of the dry air (kg)
$G_s^{\bullet}$	mass flowrate of the dry air (kg/s)
H_{cylin}, H_c, H_o	height of the cylindrical section, conical section, and stagnant bed, respectively (m)
K	global coefficient of mass transfer (m/s)
M, M_s	bed mass and mass of the dry bed (kg)
$m_v^{\bullet}$	mass flow rate of the water (kg/s)
$(Re_o)_{ms}$	Reynolds modulus corresponding to the minimum spouting velocity
T	temperature (°C)
t	time (min)
u, u_s, u_j, u_{ms}, u_{mj}	gas velocity, spouting velocity, jet-spouting velocity, minimum spouting velocity, and minimum jet-spouting velocity of the gas referred to as D_i, respectively (m/s)
V_o	bed volume (m^3)
w_D	drying rate (kg/m^2s)
X, X*	solid moisture content and equilibrium moisture content, respectively (dry basis) (kg/kg)
x_{steel}, x_{ins}	thickness of the reactor wall and insulation (m)
Y, Y_{in}, Y*	air absolute humidity, air absolute humidity at the inlet, and air absolute humidity at the equilibrium, respectively (dry basis) (kg/kg)

Greek letters

ε, ε_o	bed voidage and loose bed voidage
ϕ	sphericity, (−)
ΔP	pressure drop (Pa)
γ	angle of the contactor (deg)
μ	air viscosity (kg/m s)
ρ, ρ_s	density of the gas and of the solid, respectively (kg/m^3)

CRediT authorship contribution statement

María J. San José: Conceptualization, Data curation, Formal analysis, Funding acquisition, Investigation, Methodology, Project administration, Resources, Software, Supervision, Validation, Visualization, Writing – original draft, Writing – review & editing. **Sonia Alvarez:** Data curation, Formal analysis, Investigation, Methodology, Software, Validation, Visualization, Writing – original draft, Writing – review & editing. **Raquel López:** Data curation, Formal analysis, Investigation, Methodology, Software, Validation, Visualization, Writing – original draft, Writing – review & editing.

Declaration of competing interest

None.

Data availability

I have shared the link of my data

Acknowledgments

This work is part of the project Grant PID2021-126331OB-I00 funded by MCIN/AEI/10.13039/501100011033 and by ERDF A way of making Europe and project Grant TED2021-130150B-I00. MCIN/AEI was funded by MCIN/AEI/10.13039/501100011033 and the EU Next-GenerationEU/PRTR. The University of the Basque Country (UPV/EHU) provided open-access funding.

References

[1] International Energy Agency, World Energy Outlook, 2022.
[2] World Bioenergy Association. Global bioenergy statistics 2021. (accessed 13 July 2023) https://www.worldbioenergy.org/uploads/221223%20WBA%20GBS%202022.pdf.
[3] M. Colla, J. Blondeau, H. Jeanmart, Optimal use of lignocellulosic biomass for the energy transition, including the non-energy demand: the case of the belgian energy system, Front. Energy Res. 10 (2022) 802327, https://doi.org/10.3389/fenrg.2022.802327.
[4] M. Petitjean, N. Lamberto, A. Zornoza, J.R. Isasi, Green synthesis and chemometric characterization of hydrophobic xanthan matrices: interactions with phenolic compounds, Carbohydr. Polym. 288 (2022) 119387, https://doi.org/10.1016/j.carbpol.2022.119387.
[5] Bioenergy Europe, Biomass Supply Statistical Report, 2022 (accessed 13 July 2023) https://bioenergyeurope.org/article/396-biomass-supply-2.html.
[6] OIV, International Organisation of Vine and Wine, State of the world wine and wine sector in 2022, 2023.
[7] M. Keyser, R. Witthuhn, L.C. Ronquest, T.J. Britz, Treatment of winery effluent with upflow anaerobic sludge blanket (UASB) – granular sludges enriched with Enterobacter sakazakii, Biotechnol. Lett. 25 (2003) 1893–1898.
[8] M.T. Barcia, P.B. Pertuzatti, S. Gómez-Alonso, H.T. Godoy, I. Hermosín-Gutiérrez, Phenolic composition of grape and winemaking by-products of Brazilian hybrid cultivars BRS Violeta and BRS Lorena, Food Chem. 159 (2014) 95–105, https://doi.org/10.1016/j.foodchem.2014.02.163.
[9] J.A. Pérez-Serradilla, M.D. Luque de Castro, Role of lees in wine production: a review, Food Chem. 111 (2008) 447–456, https://doi.org/10.1016/j.foodchem.2008.04.019.
[10] Y. Carmona-Jimenez, M.V. García-Moreno, C. García-Barroso, Effect of drying on the phenolic content and antioxidant activity of red grape pomace, Plant Foods Hum. Nutr. 73 (1) (2018) 74–81, https://doi.org/10.1007/s11130-018-0658-1.
[11] M.J. San José, S. Alvarez, R. López, Conical spouted bed combustor to obtain clean energy from avocado wastes, Fuel Process. Technol. 239 (2023) 107543, https://doi.org/10.1016/j.fuproc.2022.107543.
[12] H. Li, Q. Chen, X. Zhang, K.N. Finney, V.N. Sharifi, J. Swithenbank, Evaluation of a biomass drying process using waste heat from process industries: a case study, Appl. Therm. Eng. 35 (2012) 71–80, https://doi.org/10.1016/j.applthermaleng.2011.10.009.
[13] L. Taşeri, M. Aktaş, S. Şevik, M. Gülcü, G.U. Seçkin, B. Aktekelid, Determination of drying kinetics and quality parameters of grape pomace dried with a heat pump dryer, Food Chem. 260 (2018) 152–159, https://doi.org/10.1016/j.foodchem.2018.03.122.
[14] Y. Sui, J. Yang, Q. Ye, H. Li, H. Wang, Infrared, convective, and sequential infrared and convective drying of wine grape pomace, Drying Technol. 32 (2014) 686–694, https://doi.org/10.1080/07373937.2013.853670.
[15] C. Drosou, K. Kyriakopoulou, A. Bimpilas, D. Tsimogiannis, M. Krokida, A comparative study on different extraction techniques to recover red grape pomace polyphenols from vinification by products, Ind. Crop Prod. 75 (2015) 141–149, https://doi.org/10.1016/j.indcrop.2015.05.063.
[16] A. Maskan, S. Kaya, M. Maskan, Hot air and sun drying of grape leather (pestil), J. Food Eng. 54 (2002) 81–88, https://doi.org/10.1016/S0260-8774(01)00188-1.
[17] A.M. Goula, A.N. Chasekioglou, H.N. Lazarides, Drying and shrinkage kinetics of solid waste of olive oil processing, Drying Technol. 33 (14) (2015) 1728–1738, https://doi.org/10.1080/07373937.2015.1026983.
[18] A. Martynenko, T. Kudra, Electrohydrodynamic (EHD) drying of grape pomace, Japan J. Food Eng. 17 (4) (2016) 123–129, https://doi.org/10.11301/jsfe.17.123.
[19] M. Aktaş, L. Taşeri, S. Şevik, M. Gülcü, G. Uysal Seçkin, E.C. Dolgun, Heat pump drying of grape pomace: performance and product quality analysis, Drying Technol. 37 (14) (2019) 1766–1779, https://doi.org/10.1080/07373937.2018.1536983.
[20] K. Ozkan, A. Karadag, O. Sagdic, The effects of different drying methods on the in vitro bioaccessibility of phenolics, antioxidant capacity, minerals and morphology of black 'Isabel' grape, LWT Food Sci. Technol. 158 (2022) 113185, https://doi.org/10.1016/j.lwt.2022.113185.
[21] A. Tseng, Y. Zhao, Effect of different drying methods and storage time on the retention of bioactive compounds and antibacterial activity of wine grape pomace (Pinot Noir and Merlot), J. Food Sci. 77 (9) (2012) 192–201, https://doi.org/10.1111/j.1750-3841.2012.02840.x.

[22] H. Çoklar, M. Akbulut, Effect of sun, oven and freeze-drying on anthocyanins, phenolic compounds and antioxidant activity of black grape (Ekşikara) (Vitis vinifera L.), S. Afr. J. Enol. Vitic. 38 (2) (2017) 264–272, https://doi.org/10.21548/38-2-2127.

[23] A.S.C. Teles, D.W.H. Chávez, F.S. Gomes, L.M.C. Cabral, R.V. Tonon, Effect of temperature on the degradation of bioactive compounds of pinot noir grape pomace during drying, Braz. J. Food Technol. 21 (2018) e2017059, https://doi.org/10.1590/1981-6723.5917.

[24] I.M.C. Tavares, M.B.M. Castilhos, M.A. Mauro, A.M. Ramos, R.T. Souza, S. Gómez-Alonso, E. Gomes, R. Da-Silva, I. Hermosín-Gutiérrez, E.S. Lago-Vanzela, BRS Violeta (BRS Rúbea IAC 1398-21) grape juice powder produced by foam mat drying. Part I: effect of drying temperature on phenolic compounds and antioxidant activity, Food Chem. 298 (2019) 124971, https://doi.org/10.1016/j.foodchem.2019.124971.

[25] G.V.D. da Silva, B.A.S. Machado, W.P. de Oliveira, C.F.G. da Silva, C.P. de Quadros, J.I. Druzian, E.D.S. Ferreira, M.A. Umsza-Guez, Effect of drying methods on bioactive compounds and antioxidant capacity in grape skin residues from the new hybrid variety "BRS magna", Molecules. 25 (16) (2020) 3701, https://doi.org/10.3390/molecules25163701.

[26] R. Langová, M. Jüzl, O. Cwiková, I. Kos, Effect of different method of drying of five varieties grapes (Vitis vinifera L.) on the bunch stem on physicochemical, microbiological, and sensory quality, Foods. 9 (2020) 1183, https://doi.org/10.3390/foods9091183.

[27] S.T. Suescun-Ospina, J. Avila-Stagno, N. Vera-Aguilera, R. Astudillo-Neira, I. Trujillo-Mayol, J. Alarcón-Enos, Effects of drying method on bioactive compounds contents, rumen fermentation parameters and in vitro methane output of waste dried País grape (Vitis vinifera L.) marc, Food Biosci. 51 (2023) 102154, https://doi.org/10.1016/j.fbio.2022.102154.

[28] M. Guaita, L. Panero, S. Motta, B. Mangione, A. Bosso, Effects of high temperature drying on the polyphenolic composition of skins and seeds, from red grape pomace, LWT Food Sci. Technol. 145 (2021) 111323, https://doi.org/10.1016/j.lwt.2021.111323.

[29] R.G. Fernández, C.P. García, A.G. Lavín, J.L.B. de las Heras, Study of main combustion characteristics for biomass fuels used in boilers, Fuel Process. Technol. 103 (2012) 16–26, https://doi.org/10.1016/j.fuproc.2011.12.032.

[30] M. Valente, A. Brillard, C. Schönnenbeck, J.F. Brilhac, Investigation of grape marc combustion using thermogravimetric analysis. Kinetic modeling using an extended independent parallel reaction (EIPR), Fuel Process. Technol. 131 (2015) 297–303, https://doi.org/10.1016/j.fuproc.2014.10.034.

[31] C. Schönnenbeck, G. Trouvé, M. Valente, P. Garra, J.F. Brilhac, Combustion tests of grape marc in a multi-fuel domestic boiler, Fuel 180 (2016) 324–331, https://doi.org/10.1016/j.fuel.2016.04.034.

[32] E. Benetto, C. Jury, G. Kneip, I. Vázquez-Rowe, V. Huck, F. Minette, Life cycle assessment of heat production from grape marc pellets, J. Clean. Prod. 87 (1) (2015) 149–158, https://doi.org/10.1016/j.jclepro.2014.10.028.

[33] M. Olazar, M.J. San José, F.J. Peñas, A.T. Aguayo, J. Bilbao, Stability and hydrodynamics of conical spouted beds with binary mixtures, Ind. Eng. Chem. Res. 32 (1993) 2826–2834, https://doi.org/10.1021/ie00023a053.

[34] T. Leffler, M. Eriksson, B. Leckner, F. Lind, F. Winquist, P. Knutsson, Monitoring of bed material in a biomass fluidized bed boiler using an electronic tongue, Fuel 340 (2023) 127598, https://doi.org/10.1016/j.fuel.2023.127598.

[35] M.J. San José, M. Olazar, F.J. Peñas, J. Bilbao, Segregation in conical spouted beds with binary and ternary mixtures of equidensity spherical particles, Ind. Eng. Chem. Res. 33 (1994) 1838–1844, https://doi.org/10.1021/ie00031a025.

[36] N. Epstein, K. Mathur, Heat and mass transfer in spouted beds - a review, Can. J. Chem. Eng. 49 (1971) 467–476, https://doi.org/10.1002/cjce.5450490407.

[37] K. Mathur, N. Epstein, Spouted Beds, Academic Press, New York, 1974.

[38] T. Hoffmann, A. Hailu Bedane, M. Peglow, E. Tsotsas, M. Jacob, Particle–gas mass transfer in a spouted bed with adjustable air inlet, Drying Technol. 29 (2011) 257–265, https://doi.org/10.1080/07373937.2010.483046.

[39] F.J. Peñas, B. Safont, Characterization and modeling of oxygen transfer in a spouted-bed reactor with auxiliary aeration, Chem. Eng. Technol. 40 (1) (2017) 64–70, https://doi.org/10.1002/ceat.201600100.

[40] F.J. Peñas, J.R. Isasi, Removal of cresols from water by packed beds of cyclodextrin-based hydrogels, J. Polym. Environ. 30 (3) (2022) 1189–1198, https://doi.org/10.1007/s10924-021-02259-3.

[41] N. Torres Brauer, M. Navarro Salazar, H. de Lasa, Bubbles in biomass fluidized bed gasifiers: a phenomenological probabilistic predictive model, Chem. Eng. Sci. 271 (2023) 118582, https://doi.org/10.1016/j.ces.2023.118582.

[42] M.J. San José, S. Alvarez, F.J. Peñas, I. García, Cycle time in draft tube conical spouted bed dryer for sludge from paper industry, Chem. Eng. Sci. 100 (2013) 413–420, https://doi.org/10.1016/j.ces.2013.02.058.

[43] M. Olazar, M.J. San José, A.T. Aguayo, J.M. Arandes, J. Bilbao, Stable operation conditions for gas–solid contact regimes in conical spouted beds, Ind. Eng. Chem. Res. 31 (7) (1992) 1784–1792, https://doi.org/10.1021/ie00007a025.

[44] N. Epstein, Introduction and overview, Can. J. Chem. Eng. 70 (1992) 833–835, https://doi.org/10.1002/cjce.5450700502.

[45] M.J. San José, M. Olazar, A.T. Aguayo, J.M. Arandes, J. Bilbao, Expansion of spouted beds in conical contactors, Chem. Eng. J. 51 (1) (1993) 45–52, https://doi.org/10.1016/0300-9467(93)80007-B.

[46] M.J. San José, S. Alvarez, A. Ortiz de Salazar, M. Olazar, J. Bilbao, Influence of the particle diameter and density in the gas velocity in jet spouted beds, Chem. Eng. Process. 44 (2005) 153–157, https://doi.org/10.1016/j.cep.2004.03.011.

[47] M.J. San José, S. Alvarez, A. Morales, L.B. López, A. Ortiz de Salazar, Diluted spouted bed at high temperature for the treatment of sludges wastes, Chem. Eng. Trans. 20 (2010) 303–308, https://doi.org/10.3303/CET1020051.

[48] G.K. Jayatunga, B.M.W.P.K. Amarasinghe, Drying kinetics, quality and moisture diffusivity of spouted bed dried Sri Lankan black pepper, J. Food Eng. 263 (2019) 38–45, https://doi.org/10.1016/j.jfoodeng.2019.05.023.

[49] L.P. Mussi, A.O. Guimarães, K.S. Ferreira, N.R. Pereira, Spouted bed drying of jambolão (Syzygium cumini) residue: drying kinetics and effect on the antioxidant activity, anthocyanins and nutrients contents, Food Sci. Technol. 61 (2015) 80–88, https://doi.org/10.1016/j.lwt.2014.11.040.

[50] S. Rajashekhara, D.V.R. Murthy, Drying of agricultural grains in a multiple porous draft tube spouted bed, Chem. Eng. Commun. 204 (8) (2017) 942–950, https://doi.org/10.1080/00986445.2017.1328412.

[51] M.J. San José, S. Alvarez, R. López, Drying of industrial sludge waste in a conical spouted bed dryer. Effect of air temperature and air velocity, Drying Technol. 37 (1) (2019) 118–128, https://doi.org/10.1080/07373937.2018.1441155.

[52] M.J. San José, S. Alvarez, R. López, Drying kinetics of sawdust in conical spouted beds: influence of geometric and operational factors, Fuel Process. Technol. 221 (2021) 106950, https://doi.org/10.1016/j.fuproc.2021.106950.

[53] M. Serowik, A. Figiel, M. Nejman, A. Pudlo, D. Chorazyk, W. Kopec, Drying characteristics and some properties of spouted bed dried semi-refined carrageenan, J. Food Eng. 194 (2017) 46–57, https://doi.org/10.1016/j.jfoodeng.2016.09.007.

[54] H. Duan, F. Wu, S. Zhao, X. Ma, W. Liang, T. Ding, Experimental investigation of the swirl flow enhancement effect on the particle drying process in a novel spouted bed, Ind. Eng. Chem. Res. 60 (2021) 13562–13573, https://doi.org/10.1021/acs.iecr.1c02838.

[55] T.A. Costa-Silva, A.K.F. Carvalho, C.R.F. Souza, L. Freitas, H.F. De Castro, W. P. Oliveira, Highly effective Candida rugosa lipase immobilization on renewable carriers: integrated drying and immobilization process to improve enzyme performance, Chem. Eng. Res. Des. 183 (2022) 41–55, https://doi.org/10.1016/j.cherd.2022.04.026.

[56] L. Li, H. Pan, J. Chen, W. Cao, W. Liu, X. Duan, G. Ren, Infrared-assisted spouted bed drying of Chinese yam cubes: effect of constant and variable temperature drying processes on drying behavior, uniformity and quality attributes, J. Sci. Food Agric. 103 (6) (2023) 2815–2823, https://doi.org/10.1002/jsfa.12416.

[57] S. Zhao, F. Wu, X. Ma, W. Zhou, Effect of novel intensification structure on drying of particulate materials in spouted beds, J. Ind. Eng. Chem. 114 (2022) 263–275, https://doi.org/10.1016/j.jiec.2022.07.016.

[58] D. Huang, W. Huang, S. Huang, F. Zhou, G. Gong, L. Li, B. Sunden, Applications of spouted bed technology in the drying of food products, LWT Food Sci. Technol. 182 (2023) 114880, https://doi.org/10.1016/j.lwt.2023.114880.

[59] C. Moliner, B. Bosio, E. Arato, A. Ribes, Thermal and thermo-oxidative characterization of rice straw for its use in energy valorization processes, Fuel 180 (2016) 71–79, https://doi.org/10.1016/j.fuel.2016.04.021.

[60] M.J. San José, S. Alvarez, I. García, F.J. Peñas, A novel conical combustor for thermal exploitation of vineyard pruning wastes, Fuel 110 (2013) 178–184, https://doi.org/10.1016/j.fuel.2012.10.039.

[61] M.J. San José, S. Alvarez, F.J. Peñas, I. García, Thermal exploitation of fruit tree pruning wastes in a novel conical spouted bed combustor, Chem. Eng. J. 238 (15) (2014) 227–233, https://doi.org/10.1016/j.cej.2013.09.073.

[62] M.J. San José, S. Alvarez, I. García, F.J. Peñas, Conical spouted bed combustor in clean valorization of sludge wastes from paper industry for obtaining energy, Chem. Eng. Res. Des. 92 (4) (2014) 672–678, https://doi.org/10.1016/j.cherd.2014.01.008.

[63] M.J. San José, S. Alvarez, R. López, Catalytic combustion of vineyard pruning waste in a conical spouted bed combustor, Catal. Today 305 (2018) 13–18, https://doi.org/10.1016/j.cattod.2017.11.020.

[64] H.C. Park, H.S. Choi, Fast pyrolysis of biomass in a spouted bed reactor: hydrodynamics, heat transfer and chemical reaction, Renew. Energ. 143 (2019) 1268–1284, https://doi.org/10.1016/j.renene.2019.05.072.

[65] S. Yang, R. Dong, Y. Du, S. Wang, H. Wang, Numerical study of the biomass pyrolysis process in a spouted bed reactor through computational fluid dynamics, Energy 214 (2021) 118839, https://doi.org/10.1016/j.energy.2020.118839.

[66] H. Boujjat, S. Rodat, S. Chuayboon, S. Abanades, Experimental and numerical study of a directly irradiated hybrid solar/combustion spouted bed reactor for continuous steam gasification of biomas, Energy 189 (2019) 116118, https://doi.org/10.1016/j.energy.2019.116118.

[67] F. Fan, S. Wang, S. Yang, J. Hu, H. Wang, Numerical investigation of gas thermal property in the gasification process of a spouted bed gasifier, Appl. Therm. Eng. 181 (2020) 115917, https://doi.org/10.1016/j.applthermaleng.2020.115917.

[68] S. Yang, F. Fan, J. Hu, H. Wang, Particle-scale evaluation of the biomass steam-gasification process in a conical spouted bed gasifier, renew, Energ. 162 (2020) 844–860, https://doi.org/10.1016/j.renene.2020.08.009.

[69] X. Li, P. Yan, C. Ma, J. Wang, Structural design and optimization of a solar spouted bed reactor of biomass gasification, Appl. Therm. Eng. 194 (2021) 117058, https://doi.org/10.1016/j.applthermaleng.2021.117058.

[70] M.J. San José, S. Alvarez, R. López, I. García, Development of Conical Spouted Beds technology for anaerobic digestion process of sewage sludge, in: Proceedings of 7th European Meeting on Chemical Industry and Environment. Tarragona (Spain), 2015.

[71] J.T. Freire, F.B. Freire, M.C. Ferreira, B.S. Nascimento, A hybrid lumped parameter/neural network model for spouted bed drying of pastes with inert particles, Drying Technol. 30 (11–12) (2012) 1342–1353, https://doi.org/10.1080/07373937.2012.684085.

[72] B.S. Nascimento, F.B. Freire, J.T. Freire, Neuronal and grey modelling of milk drying in spouted bed, Can. J. Chem. Eng. 91 (11) (2013) 1815–1821, https://doi.org/10.1002/cjce.21886.

[73] M.T.B. Perazzini, F.B. Freire, J.T. Freire, Influence of bed geometry on the drying of skimmed milk in a spouted bed, Adv. Chem. Eng. Sci. 5 (2015) 447–460, https://doi.org/10.4236/aces.2015.54046.
[74] Y.M. da Silva Veloso, M.M. de Almeida, O.L. Sanchez de Alsina, M.L. Passos, A. S. Mujumdar, M. Souza Leite, Hybrid phenomenological/ANN-PSO modelling of a deformable material in spouted bed drying process, Powder Technol. 366 (2020) 185–196, https://doi.org/10.1016/j.powtec.2019.12.047.
[75] M.J. San José, S. Alvarez, Bed pressure drop in conical spouted beds with a draft tube in thermal treatment of wastes of different particle diameter, density and shape, Chem. Eng. Technol. 38 (4) (2015) 709–714, https://doi.org/10.1002/ceat.201400650.
[76] M. Balakrishnan, G.S.V. Raghavan, V.V. Sreenarayanan, R. Viswanathan, Batch drying kinetics of cardamom in a two-dimensional spouted bed, Drying Technol. 29 (11) (2011) 1283–1290, https://doi.org/10.1016/j.jfoodeng.2009.08.011.
[77] L. Spreutels, B. Haut, J. Chaouki, F. Bertrand, R. Legros, Conical spouted bed drying of baker's yeast: experimentation and multi-modeling, Food Res. Int. 62 (2014) 137–150, https://doi.org/10.1016/j.foodres.2014.02.027.
[78] Y. Liu, J. Peng, Y. Kansha, M. Ishizuka, A. Tsutsumi, D. Jia, X.T. Bi, C.J. Lim, S. Sokhansanj, Novel fluidized bed dryer for biomass drying, Fuel Process. Technol. 122 (2014) 170–175, https://doi.org/10.1016/j.fuproc.2014.01.036.
[79] C. Srinivasakannan, N. Balasubramaniam, Drying of rubber wood sawdust using tray dryer, Particul. Sci. Technol. 24 (4) (2006) 427–439, https://doi.org/10.1080/02726350600934689.
[80] I. Kemp, Fundamentals of energy analysis of dryers, in: E. Tsotsas, A.S. Mujumdar (Eds.), Modern Drying Technology, 4: Energy Savings, 1st ed., Wiley-VCH Verlag GmbH & Co. KGaA, Weinheim, 2012.
[81] Y. Ghalavand, M.S. Hatamipour, A. Rahimi, Experimental and parametric study on drying of green peas in spouted bed, Int. J. Food Sci. Technol. 45 (12) (2010) 2546–2552, https://doi.org/10.1111/j.1365-2621.2010.02420.x.
[82] M. Markowski, I. Białobrzewski, A. Modrzewska, Kinetics of spouted-bed drying of barley: diffusivities for sphere and ellipsoid, J. Food Eng. 96 (2010) 380–387, https://doi.org/10.1016/j.jfoodeng.2009.08.011.
[83] D.M. Himmelblau, Accounts of experiences in the application of artificial neural networks in chemical engineering, Ind. Eng. Chem. Res. 47 (2008) 5782–5796, https://doi.org/10.1021/ie800076s.
[84] A.S. Mujumdar (Ed.), Handbook of Industrial Drying, third ed., CRC Press, Boca Raton, Florida, 2006.
[85] A. Kmiec, S. Englart, A. Ludwinska, Mass transfer during air humidification in spouted beds, Can. J. Chem. Eng. 87 (2009) 163–168, https://doi.org/10.1002/cjce.20152.